

Spawrious: A Benchmark for Fine Control of Spurious Correlation Biases

Aengus Lynch*, Gbètondji J-S Dovonon*, Jean Kaddour*, Ricardo Silva
University College London

<https://github.com/aengusl/spawrious>

Abstract

The problem of spurious correlations (SCs) arises when a classifier relies on non-predictive features that happen to be correlated with the labels in the training data. For example, a classifier may misclassify dog breeds based on the background of dog images. This happens when the backgrounds are correlated with other breeds in the training data, leading to misclassifications during test time. Previous SC benchmark datasets suffer from varying issues, e.g., over-saturation or only containing one-to-one (O2O) SCs, but no many-to-many (M2M) SCs arising between groups of spurious attributes and classes.

In this paper, we present Spawrious- $\{O2O, M2M\}$ - $\{Easy, Medium, Hard\}$, an image classification benchmark suite containing spurious correlations among different dog breeds and background locations. To create this dataset, we employ a text-to-image model to generate photo-realistic images, and an image captioning model to filter out unsuitable ones. The resulting dataset is of high quality, containing approximately 152,000 images.

Our experimental results demonstrate that state-of-the-art group robustness methods struggle with Spawrious, most notably on the Hard-splits with $< 60\%$ accuracy. By examining model misclassifications, we detect reliances on spurious backgrounds, demonstrating that our dataset provides a significant challenge to drive future research.

1. Introduction

One of the reasons we have not deployed self-driving cars and autonomous kitchen robots everywhere is their catastrophic behavior in out-of-distribution (OOD) settings that differ from the training distribution [13, 15]. To make models more robust to unseen test distributions, mitigating a classifier’s reliance on spurious, non-causal features that are not essential to the true label has attracted lots of research interest [61, 1, 31, 27]. For example, classifiers trained on ImageNet [10] have been shown to rely on back-

grounds [74, 63, 53], which are spuriously correlated with class labels but, by definition, not predictive of them.

Recent work has focused substantially on developing new methods for addressing the spurious correlations (SCs) problem [31], yet, studying and addressing the limitations of existing benchmarks remains underexplored. For example, the Waterbirds [61], and CelebA hair color [45] benchmarks remain among the most used benchmarks for the SC problem; yet, recent methods [27] achieve 97% and 92% worst-group accuracies, respectively. Such results raise the question of whether their saturation hinders meaningful methodological progression.

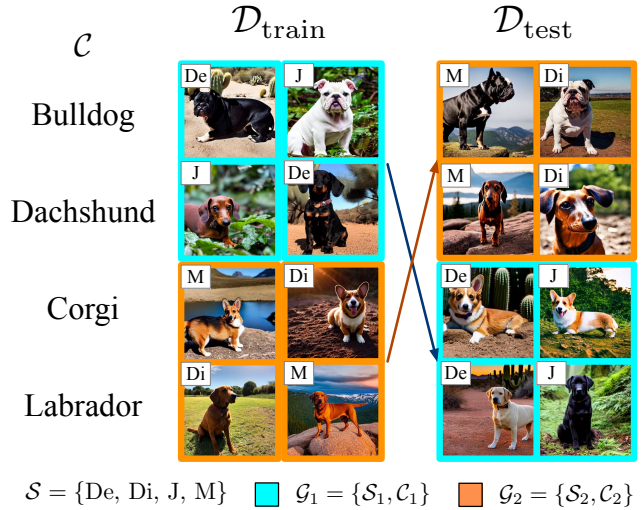


Figure 1: **Many-To-Many Spurious Correlations.** A spurious correlation exists between groups \mathcal{G} of spurious attributes \mathcal{S} and classes \mathcal{C} in the training data, which is then purposefully reversed at test time to test the classifier’s reliance on it. For example, the spurious attributes $\mathcal{S}_1 = \{\text{Desert, Jungle}\}$ correlate with $\mathcal{C}_1 = \{\text{Bulldog, Dachshund}\}$, while $\mathcal{S}_2 = \{\text{Mountain, Dirt}\}$ correlates with $\mathcal{C}_2 = \{\text{Corgi, Labrador}\}$. The upper-left labels indicate a background as one of $\mathcal{B} = \{\text{Desert, Dirt, Jungle, Mountain}\}$.

*Equal contribution, alphabetical order. ✉ aengus.lynch.17@ucl.ac.uk

Another limitation of existing benchmarks is their sole focus on overly simplistic one-to-one (O2O) spurious correlations, where one spurious attribute correlates with one label. However, in reality, we often face *many-to-many* (M2M) spurious correlations across groups of classes and backgrounds. Imagine we collect training data of animals (classes) from two locations, e.g., a tundra and a savanna, with vastly different background-label correlations. While some benchmarks include multiple training environments with varying correlations [36], they do not test classification performance when training environments are grouped, and correlations are reversed during test time. Such M2M-SCs are *not* an aggregation of O2O-SCs and cannot be expressed or decomposed in the form of the latter; they contain qualitatively different spurious structures. To the best of our knowledge, we are the first to conceptualize and instantiate M2M SCs in image classification problems.

Contributions We introduce *Spawrious*-{O2O, M2M}-{Easy, Medium, Hard}, a suite of synthetic image classification datasets with O2O and M2M spurious correlations and three difficulty levels each. Recent work [71, 47, 69] has demonstrated a proof-of-concept to effectively discover spurious correlation failure cases in classifiers by leveraging off-the-shelf, large-scale, image-to-text models trained on vast amounts of data. Here, we take this view to the extreme and generate a novel benchmark with 152,064 images of resolution 224×224 , specifically targeted at the probing of classifiers’ reliance on spurious correlations.

Our experimental results demonstrate that state-of-the-art methods struggle with *Spawrious*, most notably on the *Hard*-splits with $< 60\%$ accuracy. We probe a model’s misclassifications and find further evidence for its reliance on spurious features. We also experiment with different model architectures, finding that while larger architectures can sometimes improve performance, the gains are inconsistent across methods, further raising the need for driving future research towards solving *Spawrious*.

2. Existing Benchmarks

We summarize the differences between *Spawrious* and related benchmarks in Table 1.

DomainBed [20] is a benchmark suite consisting of seven previously published datasets focused on domain generalization (DG), not on spurious correlations (excluding CMNIST, which we discuss separately). After careful hyper-parameter tuning, the authors find that ERM, not specifically designed for DG settings, as well as DG-specific methods, perform all about the same on average. They conjecture that these datasets may comprise an ill-posed challenge. For example, they raise the question of whether DG from a photo-realistic training environment to a cartoon test environment is even possible. In contrast, we

Dataset	DG	O2O-SC	M2M-SC
CelebA-Hair Color [45]	✗	✓	✗
Waterbirds [61]	✗	✓	✗
CMNIST [1]	✓	✓	✗
DomainBed* [20]	✓	✗	✗
WILDS [36]	✓	✗	✗
NICO [78]	✓	✗	✗
MetaShift [43]	✓	✗	✗
Spawrious	✓	✓	✓

Table 1: **Differences between *Spawrious* and other benchmarks**, according to whether they pose a Domain Generalization (DG), One-To-One- and/or Many-To-Many Spurious Correlations challenge. * excluding CMNIST, which we listed separately.

follow the same rigorous hyper-parameter tuning procedure by [20] and observe stark differences among methods on *Spawrious* in Section 5.1, with ERM being the worst and 8.84% points worse than the best method on average.

WILDS [36], NICO [78] and MetaShift [43] collect in-the-wild data and group data points with environment labels. However, these benchmarks do not induce *explicit* spurious correlations between environments and labels. For example, WILDS-FMOW [36, 8] possesses a label shift between non-African and African regions; yet, the test images pose a domain generalization (DG) challenge (test images were taken several years later than training images) instead of reverting the spurious correlations observed in the training data.

Waterbirds [61], and *CelebA hair color* [45, 27] are binary classification datasets including spurious correlations but without unseen test domains (DG). Further, [26] illustrates that a simple class-balancing strategy alleviates most of their difficulty, while *Spawrious* is class-balanced from the beginning.

ColorMNIST [1] includes spurious correlations and poses a DG problem. However, it is based on MNIST and, therefore, over-simplistic, i.e., it does not reflect real-world spurious correlations involving complex background features, such as the ones found in ImageNet [63, 53].

None of the above benchmarks include explicit training and test environments for many-to-many spurious correlations.

3. Benchmark Desiderata

Motivated by the shortcomings of previous benchmarks discussed in Section 2, we want first to posit some general desiderata, which an improved benchmark dataset would satisfy. Next, we motivate and formalize the two types of spurious correlations we aim to study.

3.1. Six Desiderata

1. **Photo-realism** unlike datasets containing cartoon/sketch images [20] or image corruptions [22], which are known to conflict with current backbone network architectures [16, 17, 23], possibly confounding the evaluation of OOD algorithms.
2. **Non-binary classification problem**, to minimize accidentally correct classifications achieved by chance.
3. **Inter-class homogeneity and intra-class heterogeneity**, i.e., low variability *between* and high variability *within* classes, to minimize the margins of the decision boundaries inside the data manifold [51]. This desideratum ensures that the classification problem is non-trivial.
4. **High-fidelity backgrounds** including complex features to reflect realistic conditions typically faced in the wild instead of monotone or entirely removed backgrounds [74].
5. **Access to multiple training environments**, i.e., the conditions of the *Domain Generalization* problem [20], which allow us to learn domain invariances, such that classifiers can perform well in novel test domains.
6. **Multiple difficulty levels**, so future work can study cost trade-offs. For example, we may be willing to budget higher computational costs for methods succeeding on difficult datasets than those that succeed only on easy ones.

3.2. Spurious Correlations (One-To-One)

Here, we provide some intuition and discuss the conditions for a (one-to-one) spurious correlation (SC).

We define a correlated, non-causal feature as a feature that frequently occurs with a class but does not cause the appearance of the class (nor vice versa). We abuse the term “correlated” as it is commonly used by previous work, but we consider non-linear relationships between two random variables too. Further, we call correlated features *spurious* if the classifier perceives them as a feature of the correlated class. For example, a confounding variable, e.g., animal habitat, can cause spurious background features in animal images that are non-predictive of the animal class [31].

Next, we want to define a *challenge* that allows us to evaluate a classifier’s harmful reliance on spurious features. Spurious features are not always harmful; even humans use context information to make decisions [15]. However, a spurious feature becomes harmful if it alone is sufficient to trigger the prediction of a particular class without the class object being present in the image [53].

To evaluate a classifier w.r.t. such harmful predictions, we evaluate its performance when the spurious correla-



Figure 2: **One-To-One Spurious Correlation Challenge:** Both training groups contain a spurious correlation between each class and background, but the strength varies. *Env 1* has 97% spurious background and 3% beach background, while *Env 2* has 87% and 13% respectively. We test on unseen background-class combinations.

tions are reverted. The simplest setting is when a positive/negative correlation exists between one background variable and one label in the training/test environment. We formalize this setup as follows.

O2O-SC Challenge

Let $p(\mathbf{X}, S, Y)$ be a distribution over images $\mathbf{X} \in \mathbb{R}^D$, spurious attributes $S \in \{s_1, \dots, s_K\}$, and labels $Y \in \{c_1, \dots, c_C\}$. Given $p_{\text{train}} \neq p_{\text{test}}$, it holds that

$$\begin{aligned} \text{corr}_{p_{\text{train}}}(\mathbb{1}(S = K_i), \mathbb{1}(Y = C_j)) &> 0, \\ \text{corr}_{p_{\text{test}}}(\mathbb{1}(S = K_i), \mathbb{1}(Y = C_j)) &< 0, \end{aligned} \quad (1)$$

for some pairs $(i, j) \in [K] \times [C]$.

In a nutshell, by one-to-one (O2O) SC, we refer to a setting in which pair-wise SCs between spurious features S (also called *style* variable [31]) and labels Y exist within training environments, which then differ in the test environment. We can have O2O SCs with multiple training environments, as illustrated in Figure 2.

3.3. Many-To-Many Spurious Correlations

In this subsection, we conceptualize Many-To-Many (M2M) SCs, where the SCs hold over disjoint groups of spurious attributes and classes. For instance, in Figure 1, each class from the class group $\{\text{Bulldog}, \text{Dachshund}\}$ is observed with each background from the group $\{\text{Desert}, \text{Jungle}\}$ in equal proportion.

We believe that M2M SCs are an important generalization failure mode currently overlooked in current bench-

marks.

We emphasize that M2M-SCs are *not* an aggregation of O2O-SCs and cannot be expressed or decomposed in the form of the latter. M2M-SCs contain richer spurious structures, following an *hierarchy* of the class groups causing the spurious attributes, i.e., $C \rightarrow S$. As we will see later in Section 4.2, the data-generating processes we instantiate for each challenge differ qualitatively.

M2M-SC Challenge

Consider $p(\mathbf{X}, S, Y)$ defined in the O2O-SC Challenge. We further assume the existence of partitions $[K] = K_{A1} \dot{\cup} K_{A2}$, $[C] = C_{B1} \dot{\cup} C_{B2}$. Given $p_{\text{train}}, p_{\text{test}}$, it holds that

$$\begin{aligned} \text{corr}_{p_{\text{train}}}(\mathbb{1}(S \in K_{Ai}), \mathbb{1}(Y \in C_{Bi})) &= 1 \\ \text{corr}_{p_{\text{test}}}(\mathbb{1}(S \in K_{Ai}), \mathbb{1}(Y \in C_{Bi})) &= -1, \end{aligned} \quad (2)$$

for $i \neq j$.

4. The Spawrious Challenge

In this section, we instantiate the desiderata introduced in Section 3 by presenting *Spawrious*, a synthetic image classification dataset containing images of four dog breeds (classes) in six background locations (spurious attributes). Since we instantiate the spurious attributes with background locations, from hereon, we will denote the spurious feature S as *background* variable $b \in B$.

4.1. Dataset Construction

Figure 3 summarizes the dataset construction pipeline, which we now discuss in more detail. The main idea is to leverage recently proposed text-to-image models [59] for photo-realistic image generation and image-to-text models [55] for filtering out low-quality images.

1. A **prompt template** allows us to define high-level factors of variation, akin to a causal model [31] of the data-generating process.
2. We then **sample prompts** by filling in randomly sampled values for these high-level factors.
3. The **text-to-image model** generates images given a sampled prompt; we use *Stable Diffusion v1.4* [59].
4. We pass the raw, generated images to an **image-to-text (I2T) model** to extract a concise description; here, we use the ViT-GPT2 image captioning model [55].
5. We perform a form of **substring matching** by checking whether important keywords are present in the caption, e.g., “dog”. This step avoids including images without

class objects, which we sometimes observed due to the T2T model ignoring parts of the input prompt.

6. We **keep only “clean” images** whose captions include important keywords.

4.2. Satisfying Desiderata

As mentioned in the previous subsection, we generate images using *Stable Diffusion v1.4* [59], which was trained on a large-scale real-world image dataset [62], while carefully filtering out images without detectable class objects, thereby targeting **photorealism**.

We construct a 4-way classification problem to reduce the probability of accidentally-correct classifications compared to a **binary classification problem** (e.g., CelebA hair color prediction or Waterbirds). Next, we chose dog breeds to reduce **inter-class variance**, inspired by the difference in classification difficulty between Imagenette (easily classified objects) [24], and ImageWoof [25] (dog breeds), two datasets based on subsets of ImageNet [10]. We increase **intra-class variance** by adding animal poses to the prompt template.

We add “[location] [time of day]” variables to the prompt template to ensure **diverse backgrounds**, and select six combinations after careful experimentation with dozens of possible combinations, abandoning over-simplistic ones.

Our final prompt template takes the form “one [fur] [animal] [pose] [location], [time of day]. highly detailed, with cinematic lighting, 4k resolution, beautiful composition, hyperrealistic, trending, cinematic, masterpiece, close up”, and there are 72 possible combinations. The variables [location]/[animal] correspond to spurious backgrounds/labels for a specific background-class combination. The other variables take the following values:

- fur: black, brown, white, [empty]
- pose: sitting, running, [empty]
- time of day: pale sunrise, sunset, rainy day, foggy day, bright sunny day, bright sunny day

To construct **multiple training environments**, we randomly sample from a set of background-class combinations, which we further group by their **difficulty level into easy, medium, and hard**.

We construct two datasets for each SC type with 3168 images per background-class combination, thus $2 \text{ SC types} \times 4 \text{ environments} \times 6 \text{ difficulties} \times 3168 = 152,064$ images in total.

O2O-SC Challenge We select combinations such that each class is observed with two backgrounds, spurious b^{sp} and generic b^{ge} . For all images with class label c_i in the training data, $\mu\%$ of them have the spurious background

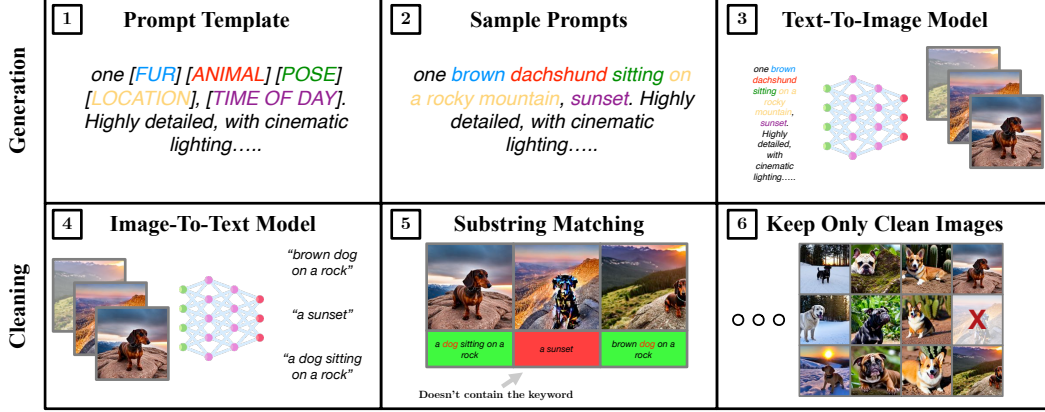


Figure 3: **Spawrious Pipeline**: We leverage text-to-image models for data generation and image-to-text models for cleaning.

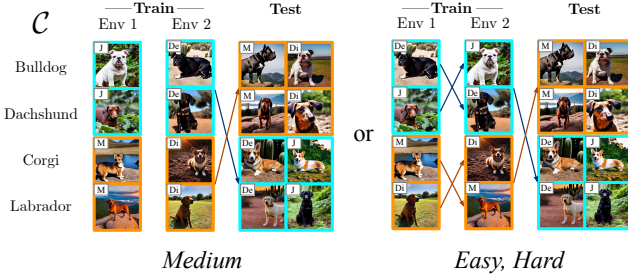


Figure 4: **Two Ways To Construct M2M-SCs**: We use the dataset shown in Figure 1 and split the training data into two environments, either with two backgrounds observed in each environment (*Medium*) or with all four (*Easy*, *Hard*). This nuance only affects environment-aware algorithms, thus does not affect the performance of ERM.

b_i^{sp} and $(100 - \mu)\%$ of them have the generic background b_i^{ge} . Importantly, each spurious background is observed with only one class ($p_{\text{train}}(b_i^{\text{sp}} | c_j) = 1$ if $i = j$ and 0 for $i \neq j$), while the generic background is observed for all classes with equal proportion. We train on two separate environments (with distinct data) that differ in their μ values. Thus, the change in this proportion should serve as a signal to the robustness algorithm that the correlation is spurious.

For instance, in Figure 2, training environment 1, 97% of the *Bulldog* images have spurious *Jungle* backgrounds, while 3% have generic *Beach* backgrounds. The spurious background changes depending on the class, but the relative proportions between each trio c_i, b_i^{sp} and b_i^{ge} are the same. Notably, in training environment 2, the proportions change to 87% and 13% split of spurious and generic backgrounds.

M2M-SC Challenge First, we construct disjoint background and class groups $\mathcal{B}_1, \mathcal{B}_2, \mathcal{C}_1, \mathcal{C}_2$, with two classes and two backgrounds, respectively. Then, we select

background-class combinations for the training data such that for each class $c \in \mathcal{C}_i$, we pick a combination (c, b) for each $b \in \mathcal{B}_i$. Second, we introduce two environments as shown in Figure 4. There are two ways to do this; where in both ways, each class is only observed with one background in an environment:

1. Each environment uses only one background from each background group (challenge *Medium* in Figure 4).
2. Each environment uses as many backgrounds as we can from each background group (challenges *Easy*, *Hard* in Figure 4).

The difference between *Easy* and *Hard* is that we randomly shuffle different background-class combinations for training and test environments and determine the final split based on a standard ERM classifier’s (Section 5) performance.

During early experimentation, we also created environments that are convex combinations of the two, which made little difference to our results. As noted in Figure 4, the choice of environments only affects environment-aware algorithms (such as IRM [1]) and does not affect ERM.

Data combination selection Each spurious correlation (O2O, M2M) comes with three data combinations (Easy, Medium, Hard) and a test environment. We selected one data combination while experimenting with ways to build spurious correlations. Those are Spawrious-{O2O}-{Easy} and Spawrious-{M2M}-{Hard} which we used for early experiments and fine-tuning. To find the remaining data combinations for Spawrious-{O2O}-{Medium, Hard} and Spawrious-{M2M}-{Easy, Medium}, we performed a random search within a space of possible data combinations for 20 random trials on O2O and M2M each. Full details on the final data combinations are here: Table 2.

Class	Train Env 1	Train Env 2	Test	Train Env 1	Train Env 2	Test	Train Env 1	Train Env 2	Test
	O2O-Easy			O2O-Medium			O2O-Hard		
Bulldog	97% De 3% B	87% De 13% B	100% Di	97% M 3% De	87% M 13% De	100% J	97% J 3% B	87% J 13% B	100% M
Dachshund	97% J 3% B	87% J 13% B	100% S	97% B 3% De	87% B 13% De	100% Di	97% M 3% B	87% M 13% B	100% S
Labrador	97% Di 3% B	87% Di 13% B	100% De	97% Di 3% De	87% Di 13% De	100% B	97% S 3% B	87% S 13% B	100% De
Corgi	97% S 3% B	87% S 13% B	100% J	97% J 3% De	87% J 13% De	100% S	97% De 3% B	87% De 13% B	100% J
	M2M-Easy			M2M-Medium			M2M-Hard		
Bulldog	100% Di	100% J	50% S 50% B	100% De	100% M	50% Di 50% J	100% B	100% S	50% De 50% M
Dachshund	100% J	100% Di	50% S 50% B	100% M	100% De	50% Di 50% J	100% B	100% S	50% De 50% M
Labrador	100% S	100% B	50% Di 50% J	100% Di	100% J	50% De 50% M	100% M	100% De	50% B 50% S
Corgi	100% B	100% S	50% Di 50% J	100% J	100% Di	50% De 50% M	100% M	100% De	50% B 50% S

Table 2: **Proportions of Spurious Backgrounds By Class and Environment.** Backgrounds include: Beach (B), Desert (De), Dirt (Di), Jungle (J), Mountain (M), Snow (S).

5. Experiments

In this section, we evaluate various group robustness methods on Spawrious and discuss the results.

Methods The field of worst-group-accuracy optimization is thriving with a plethora of proposed methods, making it impractical to compare all available methods. We choose the following six popular methods.

- **ERM** [67] refers to the canonical, average-accuracy-optimization procedure, where we treat all groups identically and ignore group labels, not targeting to improve the worst group performance.
- **CORAL** [64] penalizes differences in the first and second moment of the feature distributions of each group.
- **IRM** [1] is a causality-inspired [31] invariance-learning method, which penalizes feature distributions that have different optimal linear classifiers for each group.
- **CausIRL** [7] is another causally-motivated algorithm for learning invariances, whose penalty considers only one distance between mixtures of latent features coming from different domains.
- **GroupDRO** [61] uses Group-Distributional Robust Optimization to explicitly minimize the worst group loss instead of the average loss.
- **MMD-AAE** [42] penalizes distances between feature distributions of groups via the maximum mean discrepancy (MMD) and learning an adversarial auto-encoder (AAE).

Hyper-parameter tuning We follow the hyper-parameter tuning process used by [20] with a modification. We keep the dropout rate (0.1) and the batch size fixed (128 for ResNets and 64 for ViTs) and tune the learning rate and weight decay on ERM with a random search of 20 random trials. For all other methods, we further tune their method-specific hyper-parameters with a search of

10 random trials. We perform model selection based on the training domain validation accuracy of a subset of the training data. We reuse the hyper-parameters found for Spawrious- $\{O2O\}$ - $\{Easy\}$ and Spawrious- $\{M2M\}$ - $\{Hard\}$ on Spawrious- $\{O2O\}$ - $\{Medium, Hard\}$ and Spawrious- $\{M2M\}$ - $\{Easy, Medium\}$, respectively.

Evaluation We evaluate the classifiers on a test environment where the SCs present during training change, as described in Table 2. For O2O, multiple ways exist to choose a test data combination; we evaluate one of them as selected using a random search process. In M2M, because there are only two class groups and two background groups, we only need to swap them as seen in Figure 1.

5.1. Main Results

For our main results in Table 1, we fine-tune a ResNet18 [21] model pre-trained on ImageNet, following previous work on domain generalization [12, 41, 20]. We also fine-tune larger models later in Section 5.3.

We summarize the results as follows:

- There is a clear hierarchy among methods; the top three listed methods perform significantly worse than the bottom three. This stimulating new result contributes to the debate whether, for a fixed architecture, most robustness methods perform about the same [20] or not [72].
- The performances of most methods gets consistently worse as the challenge becomes harder.
- Most often, the data splits of our newly formalized M2M-SC are significantly more challenging than the O2O splits, most notably *M2M-Hard*. We conjecture that there is a strong need for new methods targeting such.
- $\{ERM, GroupDRO\}$ and $\{CORAL, CausIRL\}$ perform about the same, despite much different robustness regularization. The reason for this surprising result remains unclear and is left for future work.

Method	One-To-One SC			Many-To-Many SC			Average
	Easy	Medium	Hard	Easy	Medium	Hard	
ERM [68]	72.15% \pm 0.03	69.85% \pm 0.01	65.65% \pm 0.04	72.51% \pm 0.05	51.36% \pm 0.04	47.02% \pm 0.01	63.09%
GroupDRO [61]	68.72% \pm 0.02	71.87% \pm 0.01	60.90% \pm 0.03	74.82% \pm 0.04	52.06% \pm 0.03	52.79% \pm 0.03	63.53%
IRM [1]	71.26% \pm 0.02	68.18% \pm 0.02	63.78% \pm 0.03	73.28% \pm 0.04	42.43% \pm 0.07	44.51% \pm 0.06	60.57%
CORAL [64]	83.85% \pm 0.01	73.96% \pm 0.01	72.18% \pm 0.03	79.91% \pm 0.00	58.09% \pm 0.01	56.51% \pm 0.03	70.75%
CausIRL [7]	84.21%\pm0.01	73.45% \pm 0.02	71.20% \pm 0.02	81.21% \pm 0.01	56.79% \pm 0.01	56.31% \pm 0.03	70.52%
MMD-AAE [42]	82.92% \pm 0.03	74.09%\pm0.03	72.60%\pm0.05	83.45%\pm0.01	60.27%\pm0.03	58.26%\pm0.00	71.93%

Table 3: **Results for Spawrious-{O2O,M2M}-{Easy, Medium, Difficult}**, with ResNet18 pre-trained on ImageNet.

- In contrast to [66], we find no correlation between in- and out-of-distribution environment performance. All methods consistently achieve 98-99% in-distribution test performance (not shown in Table 1 to save space).
- IRM performs worst on average, with a significant difference of 11.36% compared to the best method (MMD-AAE). This result empirically confirms recent warnings about IRM’s effectiveness [60, 34].

5.2. Misclassification analysis

In Section 5.1, we learned that ERM performs particularly poorly on both hard challenges. Now, we want to investigate why by examining some of the misclassifications.

For example, we observe in Figure 5 that on the test set, the class “*Bulldog*” is misclassified as the classes whose most common training set background is the same as “*Bulldog*”’s test backgrounds. As a reminder, note that for all classes and in all data groups, both training and test environments, the number of data points per class is always balanced; rendering methods like *Subsampling large classes* [26], which achieve state-of-the-art performance on other SC benchmarks, inapplicable. Hence, we conjecture that despite balanced classes, the model heavily relies on the spurious features of the “*Mountains*” and “*Snow*” backgrounds.

We further corroborate that claim by examining the model’s confusion matrix in Figure 6. For example, Figure 6a shows the highest non-diagonal value for actual “*Dachshund*” images being wrongly classified as “*Labrador*”. We conjecture the reason being that in O2O-Hard, the background of “*Dachshund*” in the test set is “*Snow*”, which is the most common background of the training images of “*Labrador*”, as shown in Table 2.

5.3. Effect of Model Architectures

Next, we experiment with ResNet50 [21] and ViT-B/16 [11], following [27, 50]. Based on Table 4, we make the following observations:

- Scaling up to larger backbone architectures worsens the performance in three out of four cases; it only helps for

ERM, which makes it perform on par with MMD-AAE-ResNet18. However, training the ResNet50 with MMD-AAE *worsens* the performance average performance, despite us tuning its hyper-parameters for the new architecture. Similarly, the much larger ViT-B/16 backbones underperform the ResNet18 variants. The best results were obtained by the MMD-AAE, CausIRL and CORAL algorithms applied to a ResNet18. Notably, on average, a ResNet18 trained with MMD-AAE performs 1.73% better than when trained with a larger ResNet50. The ResNet18, while having the advantage of being smaller, also comes with lower standard deviations across random seeds, potentially making their training more reliable.

- In the debate on whether ViTs [11] are generally more robust to SCs [18] than CNNs or not [27, 50], our results side with the latter. We observe that a ViT-B/16 pre-trained on ImageNet22k had worse test accuracies than the ResNet architectures.

6. Related Work

Failure Mode Analyses of Distribution Shifts [52] analyze distribution shift failure modes and find that two different kinds of shifts can cause issues: *geometric* and *statistical* skew. Geometric skew occurs when there is an imbalance between groups of types of data points (i.e., data points from different environments) which induces a spurious correlation and leads to misclassification when the balance of groups changes. This understanding has motivated simply removing data points from the training data to balance between groups of data points [2]. In contrast, we study two particular types of SCs, which persist to degenerate generalization performance despite perfect balances of classes among groups.

Causality The theory of causation provides another perspective on the sources and possible mitigations of spurious correlations [56, 31]. Namely, we can formalize environment-specific data as samples from different interventional distributions, which keep the influence of variables not affected by the corresponding interventions in-

True Class of Shown Test Images: “Bulldog”

O2O-Hard: Train Data: $\text{Corr}(\text{Dachshund}, \text{Mountains}) > 0$

M2M-Hard: Train Data: $\text{Corr}(\text{Labrador}, \text{Snow}) > 0$

Misclassification: “*Dachshund*”

Misclassification: “*Labrador*”

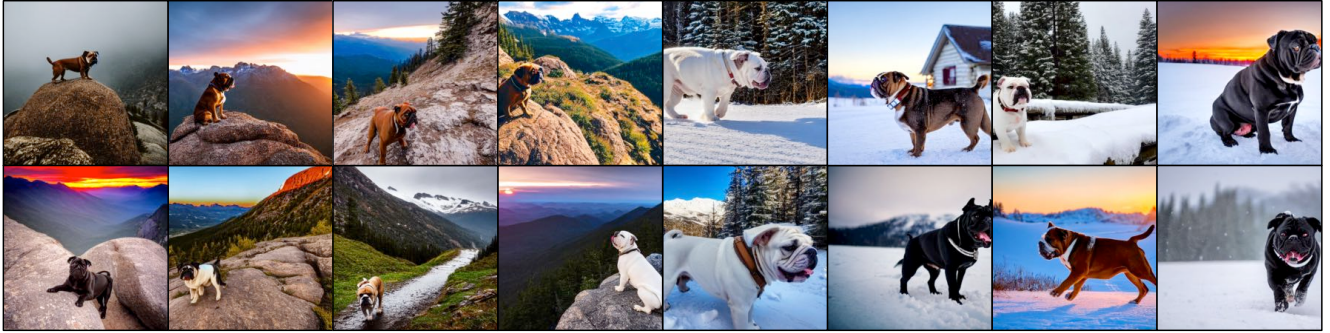


Figure 5: ERM misclassifications due to spurious correlations. The shown test images correspond to the class “Bulldog” with spurious backgrounds “Mountains” in the O2O-Hard (left) and “Snow” in the M2M-Hard (right) challenge.

Method	One-To-One SC			Many-To-Many SC			Average
	Easy	Medium	Hard	Easy	Medium	Hard	
ResNet50 (ERM)	77.49% \pm 0.05	76.60% \pm 0.02	71.32% \pm 0.09	83.80% \pm 0.01	53.05% \pm 0.03	58.70% \pm 0.04	70.16%
ResNet50 (MMD-AAE)	78.81% \pm 0.02	75.33% \pm 0.03	72.66% \pm 0.01	80.55% \pm 0.02	59.43% \pm 0.04	54.39% \pm 0.05	70.20%
ViT-B/16 (ERM)	69.06% \pm 0.05	68.58% \pm 0.01	59.38% \pm 0.02	71.46% \pm 0.02	43.16% \pm 0.03	44.99% \pm 0.02	59.44%
ViT-B/16 (MMD-AAE)	71.29% \pm 0.06	65.40% \pm 0.01	60.83% \pm 0.06	75.72% \pm 0.01	46.45% \pm 0.02	42.46% \pm 0.03	60.36%

Table 4: Effect of Different Architectures on Spawrious- $\{\text{O2O}, \text{M2M}\}$ - $\{\text{Easy}, \text{Medium}, \text{Difficult}\}$

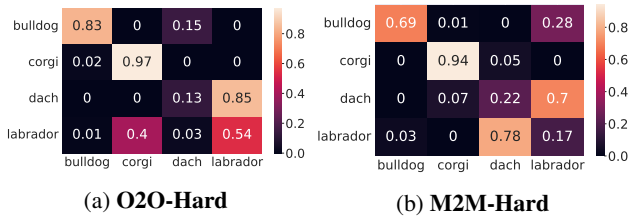


Figure 6: Confusion matrices for ERM models. True labels are on the Y-axis while predictions are on the X-axis.

variant. This perspective has motivated several invariance-learning methods that make causal assumptions on the data-generating process [1, 48, 49]. The field of causal inference also deals with mitigating spurious correlations from observational data, e.g., when estimating treatment effects [6, 38, 33, 54].

7. Limitations and Future Work

- Instantiating our desiderata with **non-background** spurious attributes. For example, [53] find that in the ImageNet [10] dataset, the class “Hard Disc” is spuriously correlated with “label”, however, “label” is not a background feature but rather part of the classification object.

- Instantiating our desiderata for **other data modalities**, e.g., text classification, leveraging the text generation capabilities of large language models [4].
- Evaluating **more generalization techniques** on Spawrious, including different robustness penalties [44, 3, 37, 5, 48, 27, 57], meta-learning [77, 9, 32, 70, 28], unsupervised domain adaptation [14, 46, 75], dropout [39], flat minima [5, 30], weight averaging [58, 73, 29], (counterfactual) data augmentation [31, 19, 76], fine-tuning of only specific layers [35, 40], diversity [65, 58], etc.

8. Conclusion

We present Spawrious, an image classification benchmark with two types of spurious correlations, one-to-one (O2O) and many-to-many (M2M). We carefully design six dataset desiderata and instantiate them by leveraging recent advances in text-to-image and image captioning models. Next, we conduct experiments and our findings indicate that even state-of-the-art group robustness techniques are insufficient in handling Spawrious, particularly in scenarios with Hard-splits where accuracy is below 60%. Our analysis of model errors revealed a dependence on irrelevant backgrounds, thus underscoring the difficulty of our dataset

and highlighting the need for further investigations in this area.

Acknowledgements

AL, GJSD, and JK acknowledge support by the Engineering and Physical Sciences Research Council with grant number EP/S021566/1.

References

- [1] Martin Arjovsky, Léon Bottou, Ishaan Gulrajani, and David Lopez-Paz. Invariant risk minimization. *arXiv preprint arXiv:1907.02893*, 2019. 1, 2, 5, 6, 7, 8
- [2] Martin Arjovsky, Kamalika Chaudhuri, and David Lopez-Paz. Throwing away data improves worst-class error in imbalanced classification. *arXiv preprint arXiv:2205.11672*, 2022. 7
- [3] Stefano B. Blumberg, Marco Palombo, Can Son Khoo, Chantal M. W. Tax, Ryutaro Tanno, and Daniel C. Alexander. Multi-stage prediction networks for data harmonization, 2019. 8
- [4] Tom Brown, Benjamin Mann, Nick Ryder, Melanie Subbiah, Jared D Kaplan, Prafulla Dhariwal, Arvind Neelakantan, Pranav Shyam, Girish Sastry, Amanda Askell, et al. Language models are few-shot learners. *Advances in neural information processing systems*, 33:1877–1901, 2020. 8
- [5] Junbum Cha, Sanghyuk Chun, Kyungjae Lee, Han-Cheol Cho, Seunghyun Park, Yunsung Lee, and Sungrae Park. Swad: Domain generalization by seeking flat minima. *Advances in Neural Information Processing Systems*, 34:22405–22418, 2021. 8
- [6] Victor Chernozhukov, Denis Chetverikov, Mert Demirer, Esther Duflo, Christian Hansen, Whitney Newey, and James Robins. Double/debiased machine learning for treatment and structural parameters, 2018. 8
- [7] Mathieu Chevalley, Charlotte Bunne, Andreas Krause, and Stefan Bauer. Invariant causal mechanisms through distribution matching. *arXiv preprint arXiv:2206.11646*, 2022. 6, 7
- [8] Gordon Christie, Neil Fendley, James Wilson, and Ryan Mukherjee. Functional map of the world, 2017. 2
- [9] Liam Collins, Aryan Mokhtari, and Sanjay Shakkottai. Task-robust model-agnostic meta-learning. *Advances in Neural Information Processing Systems*, 33:18860–18871, 2020. 8
- [10] Jia Deng, Wei Dong, Richard Socher, Li-Jia Li, Kai Li, and Li Fei-Fei. Imagenet: A large-scale hierarchical image database. In *2009 IEEE conference on computer vision and pattern recognition*, pages 248–255. Ieee, 2009. 1, 4, 8
- [11] Alexey Dosovitskiy, Lucas Beyer, Alexander Kolesnikov, Dirk Weissenborn, Xiaohua Zhai, Thomas Unterthiner, Mostafa Dehghani, Matthias Minderer, Georg Heigold, Sylvain Gelly, et al. An image is worth 16x16 words: Transformers for image recognition at scale. *arXiv preprint arXiv:2010.11929*, 2020. 7
- [12] Qi Dou, Daniel Coelho de Castro, Konstantinos Kamnitsas, and Ben Glocker. Domain generalization via model-agnostic learning of semantic features. *Advances in Neural Information Processing Systems*, 32, 2019. 6
- [13] Alexander D’Amour, Katherine Heller, Dan Moldovan, Ben Adlam, Babak Alipanahi, Alex Beutel, Christina Chen, Jonathan Deaton, Jacob Eisenstein, Matthew D Hoffman, et al. Underspecification presents challenges for credibility in modern machine learning. *Journal of Machine Learning Research*, 2020. 1
- [14] Yaroslav Ganin and Victor Lempitsky. Unsupervised domain adaptation by backpropagation. In *International conference on machine learning*, pages 1180–1189. PMLR, 2015. 8
- [15] Robert Geirhos, Jörn-Henrik Jacobsen, Claudio Michaelis, Richard Zemel, Wieland Brendel, Matthias Bethge, and Felix A Wichmann. Shortcut learning in deep neural networks. *Nature Machine Intelligence*, 2(11):665–673, 2020. 1, 3
- [16] Robert Geirhos, Patricia Rubisch, Claudio Michaelis, Matthias Bethge, Felix A Wichmann, and Wieland Brendel. Imagenet-trained cnns are biased towards texture; increasing shape bias improves accuracy and robustness. *arXiv preprint arXiv:1811.12231*, 2018. 3
- [17] Robert Geirhos, Carlos RM Temme, Jonas Rauber, Heiko H Schütt, Matthias Bethge, and Felix A Wichmann. Generalisation in humans and deep neural networks. *Advances in neural information processing systems*, 31, 2018. 3
- [18] Soumya Suvra Ghosal, Yifei Ming, and Yixuan Li. Are vision transformers robust to spurious correlations?, 2022. 7
- [19] Sven Gowal, Sylvestre-Alvise Rebuffi, Olivia Wiles, Florian Stimberg, Dan Andrei Calian, and Timothy A Mann. Improving robustness using generated data. *Advances in Neural Information Processing Systems*, 34:4218–4233, 2021. 8
- [20] Ishaan Gulrajani and David Lopez-Paz. In search of lost domain generalization. In *International Conference on Learning Representations*, 2021. 2, 3, 6
- [21] Kaiming He, Xiangyu Zhang, Shaoqing Ren, and Jian Sun. Deep residual learning for image recognition. In *Proceedings of the IEEE conference on computer vision and pattern recognition*, pages 770–778, 2016. 6, 7
- [22] Dan Hendrycks and Thomas Dietterich. Benchmarking neural network robustness to common corruptions and perturbations, 2019. 3
- [23] Katherine Hermann, Ting Chen, and Simon Kornblith. The origins and prevalence of texture bias in convolutional neural networks. *Advances in Neural Information Processing Systems*, 33:19000–19015, 2020. 3
- [24] Jeremy Howard. Imagenette: A smaller subset of 10 easily classified classes from imagenet, March 2019. 4
- [25] Jeremy Howard. Imagewoof: a subset of 10 classes from imagenet that aren’t so easy to classify, March 2019. 4
- [26] Badr Youbi Idrissi, Martin Arjovsky, Mohammad Pezeshki, and David Lopez-Paz. Simple data balancing achieves competitive worst-group-accuracy. In *Conference on Causal Learning and Reasoning*, pages 336–351. PMLR, 2022. 2, 7
- [27] Pavel Izmailov, Polina Kirichenko, Nate Gruver, and Andrew Gordon Wilson. On feature learning in the presence of spurious correlations. *arXiv preprint arXiv:2210.11369*, 2022. 1, 2, 7, 8

- [28] Penghao Jiang, Ke Xin, Zifeng Wang, and Chunxi Li. Invariant meta learning for out-of-distribution generalization. *arXiv preprint arXiv:2301.11779*, 2023. 8
- [29] Jean Kaddour. Stop wasting my time! saving days of imagenet and BERT training with latest weight averaging. In *Has it Trained Yet? NeurIPS 2022 Workshop*, 2022. 8
- [30] Jean Kaddour, Linqing Liu, Ricardo Silva, and Matt Kusner. When do flat minima optimizers work? In Alice H. Oh, Alekh Agarwal, Danielle Belgrave, and Kyunghyun Cho, editors, *Advances in Neural Information Processing Systems*, 2022. 8
- [31] Jean Kaddour, Aengus Lynch, Qi Liu, Matt J. Kusner, and Ricardo Silva. Causal machine learning: A survey and open problems. *arXiv preprint arXiv:2206.15475*, 2022. 1, 3, 4, 6, 7, 8
- [32] Jean Kaddour, Steindor Saemundsson, and Marc Deisenroth (he/him). Probabilistic Active Meta-Learning. In H. Larochelle, M. Ranzato, R. Hadsell, M. F. Balcan, and H. Lin, editors, *Advances in Neural Information Processing Systems*, volume 33, pages 20813–20822. Curran Associates, Inc., 2020. 8
- [33] Jean Kaddour, Yuchen Zhu, Qi Liu, Matt J Kusner, and Ricardo Silva. Causal effect inference for structured treatments. *Advances in Neural Information Processing Systems*, 34:24841–24854, 2021. 8
- [34] Pritish Kamath, Akilesh Tangella, Danica Sutherland, and Nathan Srebro. Does invariant risk minimization capture invariance? In *International Conference on Artificial Intelligence and Statistics*, pages 4069–4077. PMLR, 2021. 7
- [35] Polina Kirichenko, Pavel Izmailov, and Andrew Gordon Wilson. Last layer re-training is sufficient for robustness to spurious correlations. *arXiv preprint arXiv:2204.02937*, 2022. 8
- [36] Pang Wei Koh, Shiori Sagawa, Henrik Marklund, Sang Michael Xie, Marvin Zhang, Akshay Balsubramani, Weihua Hu, Michihiro Yasunaga, Richard Lanus Phillips, Irena Gao, et al. Wilds: A benchmark of in-the-wild distribution shifts. In *International Conference on Machine Learning*, pages 5637–5664. PMLR, 2021. 2
- [37] David Krueger, Ethan Caballero, Joern-Henrik Jacobsen, Amy Zhang, Jonathan Binas, Dinghui Zhang, Remi Le Priol, and Aaron Courville. Out-of-distribution generalization via risk extrapolation (rex). In *International Conference on Machine Learning*, pages 5815–5826. PMLR, 2021. 8
- [38] Sören R Künnel, Jasjeet S Sekhon, Peter J Bickel, and Bin Yu. Metalearners for estimating heterogeneous treatment effects using machine learning. *Proceedings of the national academy of sciences*, 116(10):4156–4165, 2019. 8
- [39] Tyler LaBonte, Vidya Muthukumar, and Abhishek Kumar. Dropout disagreement: A recipe for group robustness with fewer annotations. In *NeurIPS 2022 Workshop on Distribution Shifts: Connecting Methods and Applications*, 2022. 8
- [40] Yoonho Lee, Annie S. Chen, Fahim Tajwar, Ananya Kumar, Huaxiu Yao, Percy Liang, and Chelsea Finn. Surgical Fine-Tuning Improves Adaptation to Distribution Shifts, Mar. 2023. *arXiv:2210.11466 [cs]*. 8
- [41] Da Li, Jianshu Zhang, Yongxin Yang, Cong Liu, Yi-Zhe Song, and Timothy M Hospedales. Episodic training for domain generalization. In *Proceedings of the IEEE/CVF International Conference on Computer Vision*, pages 1446–1455, 2019. 6
- [42] Haoliang Li, Sinno Jialin Pan, Shiqi Wang, and Alex C Kot. Domain generalization with adversarial feature learning. In *Proceedings of the IEEE conference on computer vision and pattern recognition*, pages 5400–5409, 2018. 6, 7
- [43] Weixin Liang and James Zou. Metashift: A dataset of datasets for evaluating contextual distribution shifts and training conflicts. In *International Conference on Learning Representations*, 2022. 2
- [44] Evan Z Liu, Behzad Haghighi, Annie S Chen, Aditi Raghunathan, Pang Wei Koh, Shiori Sagawa, Percy Liang, and Chelsea Finn. Just train twice: Improving group robustness without training group information. In *International Conference on Machine Learning*, pages 6781–6792. PMLR, 2021. 8
- [45] Ziwei Liu, Ping Luo, Xiaogang Wang, and Xiaoou Tang. Deep learning face attributes in the wild. In *Proceedings of the IEEE international conference on computer vision*, pages 3730–3738, 2015. 1, 2
- [46] Mingsheng Long, Han Zhu, Jianmin Wang, and Michael I Jordan. Unsupervised domain adaptation with residual transfer networks. *Advances in neural information processing systems*, 29, 2016. 8
- [47] Aengus Lynch, Jean Kaddour, and Ricardo Silva. Evaluating the impact of geometric and statistical skews on out-of-distribution generalization performance. In *NeurIPS 2022 Workshop on Distribution Shifts: Connecting Methods and Applications*, 2022. 2
- [48] Divyat Mahajan, Shruti Tople, and Amit Sharma. Domain generalization using causal matching. In *International Conference on Machine Learning*, pages 7313–7324. PMLR, 2021. 8
- [49] Chengzhi Mao, Kevin Xia, James Wang, Hao Wang, Junfeng Yang, Elias Bareinboim, and Carl Vondrick. Causal transportability for visual recognition. In *Proceedings of the IEEE/CVF Conference on Computer Vision and Pattern Recognition*, pages 7521–7531, 2022. 8
- [50] Raghav Mehta, Vitor Albiero, Li Chen, Ivan Evtimov, Tamar Glaser, Zhiheng Li, and Tal Hassner. You only need a good embeddings extractor to fix spurious correlations. *arXiv preprint arXiv:2212.06254*, 2022. 7
- [51] Kevin P. Murphy. *Probabilistic Machine Learning: An introduction*. MIT Press, 2022. 3
- [52] Vaishnavh Nagarajan, Anders Andreassen, and Behnam Neyshabur. Understanding the failure modes of out-of-distribution generalization, 2020. 7
- [53] Yannic Neuhäus, Maximilian Augustin, Valentyn Boreiko, and Matthias Hein. Spurious features everywhere – large-scale detection of harmful spurious features in imagenet, 2022. 1, 2, 3, 8
- [54] Xinkun Nie and Stefan Wager. Quasi-oracle estimation of heterogeneous treatment effects. *Biometrika*, 108(2):299–319, 2021. 8

- [55] NLP Connect. vit-gpt2-image-captioning (revision 0e334c7), 2022. 4
- [56] Jonas Peters, Dominik Janzing, and Bernhard Schölkopf. *Elements of causal inference: foundations and learning algorithms*. The MIT Press, 2017. 7
- [57] Alexandre Rame, Corentin Dancette, and Matthieu Cord. Fishr: Invariant gradient variances for out-of-distribution generalization. In *International Conference on Machine Learning*, pages 18347–18377. PMLR, 2022. 8
- [58] Alexandre Rame, Matthieu Kirchmeyer, Thibaud Rahier, Alain Rakotomamonjy, Patrick Gallinari, and Matthieu Cord. Diverse weight averaging for out-of-distribution generalization. *arXiv preprint arXiv:2205.09739*, 2022. 8
- [59] Robin Rombach, Andreas Blattmann, Dominik Lorenz, Patrick Esser, and Björn Ommer. High-resolution image synthesis with latent diffusion models. In *Proceedings of the IEEE/CVF Conference on Computer Vision and Pattern Recognition*, pages 10684–10695, 2022. 4
- [60] Elan Rosenfeld, Pradeep Ravikumar, and Andrej Risteski. The risks of invariant risk minimization. *arXiv preprint arXiv:2010.05761*, 2020. 7
- [61] Shiori Sagawa, Pang Wei Koh, Tatsunori B. Hashimoto, and Percy Liang. Distributionally robust neural networks for group shifts: On the importance of regularization for worst-case generalization, 2019. 1, 2, 6, 7
- [62] Christoph Schuhmann, Romain Beaumont, Richard Vencu, Cade Gordon, Ross Wightman, Mehdi Cherti, Theo Coombes, Aarush Katta, Clayton Mullis, Mitchell Wortsman, Patrick Schramowski, Srivatsa Kundurthy, Katherine Crowson, Ludwig Schmidt, Robert Kaczmarczyk, and Jenia Jitsev. Laion-5b: An open large-scale dataset for training next generation image-text models, 2022. 4
- [63] Sahil Singla and Soheil Feizi. Salient imagenet: How to discover spurious features in deep learning? *arXiv preprint arXiv:2110.04301*, 2021. 1, 2
- [64] Baochen Sun and Kate Saenko. Deep coral: Correlation alignment for deep domain adaptation. In *Computer Vision—ECCV 2016 Workshops: Amsterdam, The Netherlands, October 8–10 and 15–16, 2016, Proceedings, Part III 14*, pages 443–450. Springer, 2016. 6, 7
- [65] Damien Teney, Ehsan Abbasnejad, Simon Lucey, and Anton Van den Hengel. Evading the simplicity bias: Training a diverse set of models discovers solutions with superior ood generalization. In *Proceedings of the IEEE/CVF Conference on Computer Vision and Pattern Recognition*, pages 16761–16772, 2022. 8
- [66] Damien Teney, Yong Lin, Seong Joon Oh, and Ehsan Abbasnejad. Id and ood performance are sometimes inversely correlated on real-world datasets. *arXiv preprint arXiv:2209.00613*, 2022. 7
- [67] Vladimir Vapnik. Principles of risk minimization for learning theory. *Advances in neural information processing systems*, 4, 1991. 6
- [68] Vladimir Vapnik. Principles of risk minimization for learning theory. *Advances in neural information processing systems*, 4, 1991. 7
- [69] Joshua Vendrow, Saachi Jain, Logan Engstrom, and Aleksander Madry. Dataset interfaces: Diagnosing model failures using controllable counterfactual generation. *arXiv preprint arXiv:2302.07865*, 2023. 2
- [70] Zhenyi Wang, Tiehang Duan, Le Fang, Qiuling Suo, and Mingchen Gao. Meta learning on a sequence of imbalanced domains with difficulty awareness. In *Proceedings of the IEEE/CVF International Conference on Computer Vision*, pages 8947–8957, 2021. 8
- [71] Olivia Wiles, Isabela Albuquerque, and Sven Gowal. Discovering bugs in vision models using off-the-shelf image generation and captioning. *arXiv preprint arXiv:2208.08831*, 2022. 2
- [72] Olivia Wiles, Sven Gowal, Florian Stimberg, Sylvestre Alvisé-Rebuffi, Ira Ktena, Krishnamurthy Dvijotham, and Taylan Cemgil. A fine-grained analysis on distribution shift. *arXiv preprint arXiv:2110.11328*, 2021. 6
- [73] Mitchell Wortsman, Gabriel Ilharco, Samir Ya Gadre, Rebecca Roelofs, Raphael Gontijo-Lopes, Ari S Morcos, Hongseok Namkoong, Ali Farhadi, Yair Carmon, Simon Kornblith, et al. Model soups: averaging weights of multiple fine-tuned models improves accuracy without increasing inference time. In *International Conference on Machine Learning*, pages 23965–23998. PMLR, 2022. 8
- [74] Kai Xiao, Logan Engstrom, Andrew Ilyas, and Aleksander Madry. Noise or signal: The role of image backgrounds in object recognition. *arXiv preprint arXiv:2006.09994*, 2020. 1, 3
- [75] Tongkun Xu, Weihua Chen, Pichao Wang, Fan Wang, Hao Li, and Rong Jin. Cdtrans: Cross-domain transformer for unsupervised domain adaptation. *arXiv preprint arXiv:2109.06165*, 2021. 8
- [76] Huaxiu Yao, Yu Wang, Sai Li, Linjun Zhang, Weixin Liang, James Zou, and Chelsea Finn. Improving Out-of-Distribution Robustness via Selective Augmentation. In *Proceedings of the 39th International Conference on Machine Learning*, pages 25407–25437. PMLR, June 2022. ISSN: 2640-3498. 8
- [77] Marvin Zhang, Henrik Marklund, Abhishek Gupta, Sergey Levine, and Chelsea Finn. Adaptive risk minimization: A meta-learning approach for tackling group shift. *arXiv preprint arXiv:2007.02931*, 8:9, 2020. 8
- [78] Xingxuan Zhang, Yue He, Tan Wang, Jiaxin Qi, Han Yu, Zimu Wang, Jie Peng, Renzhe Xu, Zheyang Shen, Yulei Niu, et al. Nico challenge: Out-of-distribution generalization for image recognition challenges. In *European Conference on Computer Vision*, pages 433–450. Springer, 2023. 2